SUBSURFACE STRUCTURES OF LARGE VOLCANIC COMPLEXES ON THE NEARSIDE OF THE MOON. Q. Huang, Z. Xiao and L. Xiao, Planetary Science Institute, China University of Geosciences (388 Lumo Road, Wuhan, 430074, China, qianhuang@cug.edu.cn)

Introduction: The NASA Gravity Recovery and Interior Laboratory (GRAIL) mission has mapped the lunar gravity field with unprecedentedly high resolution [1]. The up-to-date 660 degrees and orders gravity model has a spatial resolution better than 15 km [2], which is sufficient at resolve large volcanic complexes on the Moon. These features have long been popular targets for lunar geological and geochemical investigations due to their unique volcanic features. Using high-resolution imagery and topographic data returned by the Lunar Reconnaissance Orbiter (LRO), Spudis et al. [3] proposed eight large lunar volcanic complexes as shield volcanoes on the lunar nearside, of which six are located within the Oceanus Procellarum and two are in the eastern Mare Tranquillitatis (Figure 1). They are generally located at regionally high elevations and with relatively well-localized gravity anomalies, making it possible to analyze their interior structures. Combining GRAIL gravity data and LRO topography data, we carry out both localized spectral analyses and band-limited Bouguer gravity for those volcanic complexes to comprehensively study their subsurface structures.

Subsurface structures from localized spectral analyses: Mass density is important to determine the composition of a volcano, which is useful for understanding crustal evolution. Elastic thickness is related with thermal evolution of a planet and loading ratio is crucial to identify subsurface structures. We try to constrain crustal densities, volcanic load densities, elastic lithosphere thicknesses, and loading ratios for the eight proposed large shield volcanoes [3] by using localized admittance analyses.

Observed admittance spectra are interpreted in terms of a thin elastic lithospheric model that considers both surface and subsurface loads. In the gravity modeling, Young's modulus and Poisson's ratio are set to be constants, and the crustal thickness is set to the average value predicted by the recent crustal thickness model of Wieczorek et al. [4]. In the case of deriving load densities, we set the crustal density to be 2550 kg m^{-3}, which is the average density of the lunar crust derived from the GRAIL [4].

The spherical gravity and topography models are truncated to degree 330 according to the observation resolution [2]. Since our lithosphere flexure models require nearly unique correlations, we choose regions whose admittance spectra are available for analyzing. The Prinz and Cauchy complexes have been excluded in this study due to their inconsistent low correlations in their localized degree ranges. We make a gridded search for the rest six volcanic complexes and constrain their best-fit geophysical parameters.

Modeled admittances and their best-fit parameters are shown in Figure 2. The crustal and load densities of Rümker Hills, Gardner, Kepler and Marius Hills are generally larger than that of the highland crust, varying from 2850 to 3300 kg m^{-3}. Positive loading ratios of Rümker Hills and Gardner suggest dense materials beneath them. However, both Aristarchus and Hortensius have relative low crustal and load densities of ~2500 to 2600 kg m^{-3}, which are consistent with the mean density of the lunar highland crust. Small loading ratios of these two complexes indicate negligible subsurface loads. The elastic thicknesses are less constrained than densities but generally with small values, indicating a thin lithosphere of lunar volcanic complexes regions.

Subsurface structures from Band-limited Bouguer gravity: Localized spectral analyses provide a useful way to constrain the densities of the volcanic complexes, but this technique is hard to resolve how materials vary with depth in concentration. Therefore, we use the band-limited Bouguer gravity (BBG) [5] to study the regional and near surface mass concentrations for those volcanic complexes.

We select represent spherical harmonic degrees to calculate the accumulating anomalies for each region. As shown in Figure 3, Rümker Hills, Gardner, Prinz and Marius Hills all show positive Bouguer gravity anomalies at depth which are well related with surface topographies. This suggests possible dense materials such as solidified magmas may occur in the subsurface. Gardner is a typical example of this type of volcanic complexes, which exhibits a strong positive anomaly at a shallow crustal depth within 12 km. The anomaly signal seems increasing with depths before reaching a topography-equaled shape at the depth of 72 km. Long wavelength negative anomalies at deeper depth reduce the amplitude of the positive signals. Marius Hills posses the same features of Gardner, but with almost no obvious positive anomaly at the shallow depth of 12 km. Rümker Hills has a small positive anomaly at a shallow depth within 12 km which corresponds to its highest southern topography. This signal quickly increases in both amplitude and shape, which is consistent with the topography. Prinz shares the same characteristics as the Rümker Hills.

However, there are almost no obvious topography-related positive anomalies beneath Kepler, Aristarchus, Hortensius or Cauchy within depths of crust (about 35 km), suggesting that no major dense material is accumulated beneath these volcanic complexes. Alternatively, there are possible shallow magma reservoirs beneath those regions (e.g., dikes and laccolith), which may be too narrow to be distinguished in our BBG map due to the resolution limitations of the gravity filed.

Conclusions: Combining recent gravity data obtained by GRAIL and topography data obtained by LRO, we use both localized admittance analyses and band-limited Bouguer gravity to study the subsurface structures for the eight large volcanic complexes on the nearside of the Moon. Localized admittance analyses suggest that dense material that may be surface lava occur at Rümker Hills, Gardner, Kepler and Marius Hills, whereas the surface of Aristarchus Plateau and Hortensius has low bulk density which is almost the same as that of the lunar highland crust. Band-limited Bouguer gravity data show that solidified dense units occur at the surface of Rümker Hills, Gardner, Prinz, and Marius Hills, but no obvious subsurface loads occur beneath Kepler, Aristarchus, Hortensius or Cauchy.

Our results on Marius Hills and Aristarchus Plateau are consistent with previous studies [6, 7] that used longer wavelength (lower resolution) gravity models.

References: [1] Zuber M. A. et al. (2013) *Science*, *339*, 668-671. [2] Konopliv A. S. et al. (2013) *JGR-Planets, 118*, 1415-1434. [3] Spudis P. D. et al. (2013) *JGR-Planets, 118*, 1063-1081. [4] Wieczorek M. A. et al. (2013) *Science*, *339*, 671-675. [5] Featherstone W. E. et al. (2013) *JGR-Planets, 118*, 1-17. [6] Kiefer W. S. (2013) *JGR-Planets, 118*, 733-745. [7] Huang Q. et al. (2013) *PSS, 89*, 188-193.

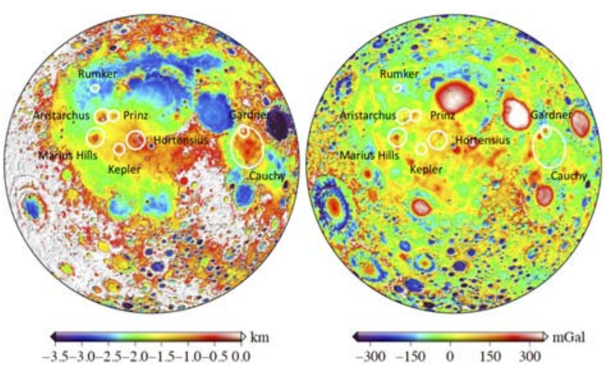

Figure 1. Topography (Left) and gravity map (Right) of the lunar nearside. The topography is derived from LOLA and the free-air gravity is from the newly released GL0660B gravity model, both the topography and gravity models are referenced to a lunar sphere radius of 1738.0 km and are truncated at spherical harmonic degree 330. The white circles indicate the area of recently proposed large shield volcanoes by [3]. Both panels are centered at 0°N, 340°E with a Lambert Azimuthal equal area projection.

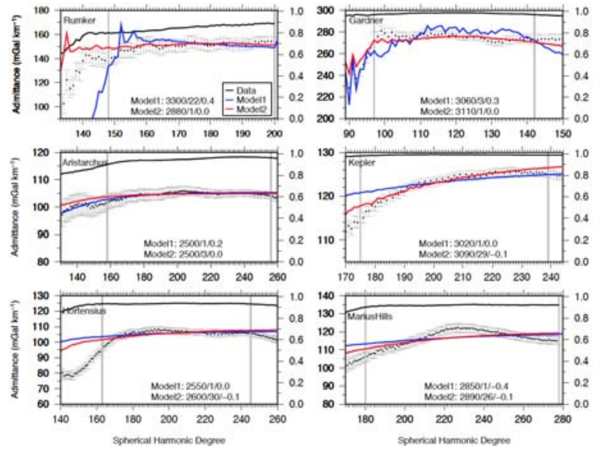

Figure 2. Analyzed admittances (black dots) and correlations (black curves) for six volcanoes. The best-fitting parameters values are given as Model 1 (blue; crustal-density/elastic-thickness/loading-ratio), and Model 2 (red; load-density/elastic-thickness/loading-ratio. Vertical gray lines indicate analyzed misfit ranges for each region.

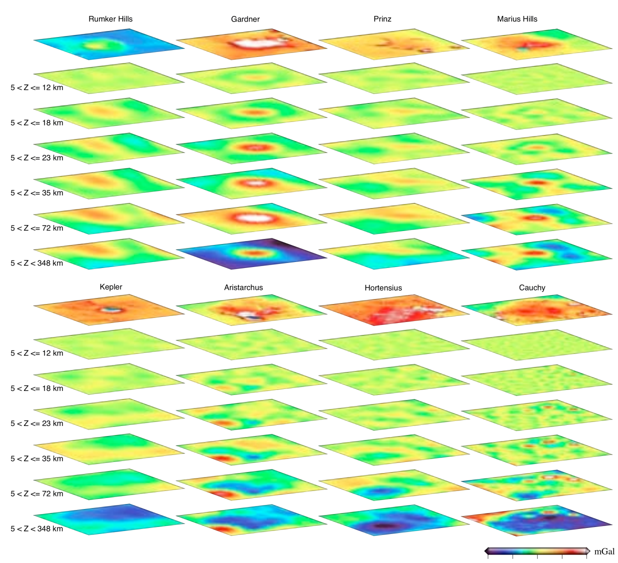

Figure 3. Band-limited Bouguer gravity anomalies of the eight volcanic complexes at different accumulating depths. The maximum depths of 5, 12, 18, 23, 35, 72 and 348 km represent band degrees of 330, 150, 100, 75, 50, 25, and 6, respectively. The top layer is the LOLA topography map. The figures are in cylindrical equidistant projections, and looked at the surface from SE at 12-degree elevation.